

CEBAF PROPOSAL COVER SHEET

This Proposal must be mailed to:

CEBAF  
Scientific Director's Office  
12000 Jefferson Avenue  
Newport News, VA 23606

and received on or before OCTOBER 30, 1989

A. TITLE: Investigation of the Spin Dependence of the AN Effective Interaction in the P Shell

B. CONTACT PERSON: Ed V. Hungerford, **LG TAB**

ADDRESS, PHONE AND BITNET:

Dept. of Physics, University of Houston, Houston, TX77204-5504  
(713) 749-3843 HUNGER@UHRCC

C. THIS PROPOSAL IS BASED ON A PREVIOUSLY SUBMITTED LETTER OF INTENT

YES  
 NO

IF YES, TITLE OF PREVIOUSLY SUBMITTED LETTER OF INTENT

Same as above

D. ATTACH A SEPARATE PAGE LISTING ALL COLLABORATION MEMBERS AND THEIR INSTITUTIONS

===== (CEBAF USE ONLY) =====

Letter Received 10-30-89

Log Number Assigned PR-89-009

By KES

contact: Hungerford

INVESTIGATION OF THE SPIN DEPENDENCE  
OF THE  $\Lambda$ N EFFECTIVE INTERACTION  
IN THE P SHELL

Participants

University of Houston  
E. V. Hungerford(Spokesman), B. W. Mayes, R. Phelps,  
L. S. Pinsky, L. G. Tang, Graduate Students

Brookhaven National Laboratory  
S. Bart, R. E. Chrien(Alternate Spokesman), P. Pile, R. Sutter

Florida State University  
L. C. Dennis, K. W. Kemper

North Carolina State University  
S. R. Cotanch

University of Mississippi  
J. J. Reidy

University of New Hampshire  
J. Wise

Abstract

We propose to investigate the spin doublet splittings in p shell hypernuclei in order to further determine the effective  $\Lambda$ N interaction. Although previous investigations have shown that the  $\Lambda$  spin orbit strength is small, a full parameter set for the  $\Lambda$ -N effective interaction is not well defined. As an initial series of experiments in the electroproduction of strangeness, we propose to study the spectroscopy of several p shell hypernuclei, attempting to observe the spin doublet splittings. Direct observation of the energy differences between these levels should help to uniquely define the effective  $\Lambda$ -N interaction.

## I. Introduction

This proposal emphasizes that the physics of strange nuclear systems may address fundamental issues that should shed light on our current understanding of hadronic many body systems, and that these issues can be explored at CEBAF. In fact the features of CEBAF, including beam quality, as well as the properties of the electromagnetic interaction can provide unique information not attainable at other facilities.

However, because of the weak spin dependence of the lambda, splitting of levels within major shell orbits will be small.<sup>1</sup> A recent ( $\pi, k$ ) reaction populating hypernuclei in heavier A targets shows strong reaction strength to a series of particle-hole states deeply embedded within the nucleus.<sup>2</sup> In effect the reaction removes a valance neutron and replaces it with a lambda in any of the lower shell orbitals within the nucleus. This series of levels may be analyzed to determine if a repulsive Pauli pressure affects the level positions, particularly in heavy systems.<sup>3</sup> Although the present fit to the data shows no evidence of unusual behavior it has been pointed out that the difference between this fit and a shift to be expected from partial quark deconfinement, would be about 1.5 MeV for the 1s shell in Pb.<sup>4</sup> The expected magnitude of the shift points out that one must precisely measure the level structure of many heavy hypernuclei to extract such information.

In addition, the effective interaction potential for p shell hypernuclei predicts various level splittings, and in particular those within a given spin multiplit.<sup>5</sup> This interaction predicts doublet splittings of order 100 to 200 keV. However, the parameter set is not without difficulties.<sup>6</sup> High resolution data is needed to identify transitions to specific levels. Present spectra using hadronic beams are limited to resolutions of about 2MeV FWHM. The quality of the beam at CEBAF offers the unique possibility of obtaining spectra with an order of magnitude better resolution.

## II. Background

Lambda hypernuclear structure is best understood in the weak coupling model. In this model the lambda hyperon replaces one of the nucleons creating a set of lambda particle - nucleon hole states.

Although not correct in detail, because the residual interaction mixes the levels,<sup>7</sup> the model still explains the gross features of the spectra. Thus, the lowest excitations of the nuclear core are added to a lambda in the l=0 shell to obtain the lowest hypernuclear excitations. In general for angular momentum of the core, j, not equal to zero, two hypernuclear levels with  $j \pm 1/2$  are created. The splitting of these levels obviously measures the spin dependence of the lambda-nucleus interaction.

The lambda-nucleon two body interaction may be parameterized as:<sup>5</sup>

$$V_{\Lambda N}(r) = V_0(r) + V_\sigma(r)\vec{S} \cdot \vec{S} + V_\Lambda \vec{L}_{N\Lambda} \cdot \vec{S}_\Lambda + V_N(r)\vec{L}_{N\Lambda} \cdot \vec{S}_N + V_T(r)S_{12};$$

where  $\vec{L}_{N\Lambda}$  is the relative orbital angular momentum, and  $S_{12}$  the tensor operator;

$$S_{12} = 3(\vec{\sigma}_N \cdot \hat{r})(\vec{\sigma}_\Lambda \cdot \hat{r}) - \vec{\sigma}_N \cdot \vec{\sigma}_\Lambda$$

and  $\vec{r} = \vec{r}_N - \vec{r}_\Lambda$ . This two body interaction may be turned into an effective lambda - nucleus potential by diagonalizing a set of shell model states. The spin doublet splittings are then given by:

$$\delta = 2/3\Delta + 4/3S_\Lambda - 8/5T;$$

at the beginning of the p shell and;

$$\delta = -1/3\Delta + 4/3S_\Lambda - 8T;$$

at the end of the shell. Here  $\Delta$  is the effective spin-spin parameter,  $S_\Lambda$  is the effective lambda spin orbit parameter, and T the effective tensor parameter. In addition to these parameters, an average central parameter  $\tilde{V}$ , and an induced spin orbit parameter  $S_N$  are needed to complete the parameter set. A review of the effective parameters is given in Reference 5. It is worthwhile to note that  $\Delta$ , and T are not measured for the p shell, but rely on theoretical estimates or extrapolations. The tensor term is seen to have little effect except for the heaviest p shell nuclei. Some typical predicted splittings are shown in Fig. 1.

Earlier work has shown that the spin orbit term,  $S_\Lambda$ , is small,<sup>1</sup> with the limit on the magnitude of this term determined by the inability to resolve the splitting of the 3 MeV gamma ray from the first excited doublet of  ${}^9\text{Be}$  to the ground state.<sup>8</sup> More recent work has attempted to find the predicted 170 keV gamma transition in  ${}^{10}_\Lambda\text{B}$  using an intrinsic Ge detector with resolution of 6 keV.<sup>12</sup> No such hypernuclear transitions

were observed between 80 to 511 keV at a factor of 4 below the predicted excitation strength. Thus, either the doublet has splitting below 80 keV, or the structure calculations are in error. In order to reduce the splitting below 80 keV the spin-spin term would need to be reduced by at least a factor of 2. However, such a value would then be inconsistent with the value needed to predict the mass difference between the ground states of the hypernuclei,  ${}^7_{\Lambda}\text{Li}$  and  ${}^7_{\Lambda}\text{Be}$ .

It is possible that a consistent set of effective parameters cannot be found for the p shell. Since the lambda and sigma couple strongly in the nucleus, it has been proposed that the lambda potential is strongly isospin dependent.<sup>9</sup> It is, in fact, known that the charge symmetry breaking term in the lambda interaction is much more important than for the nucleon.<sup>10</sup> Thus, lambda-sigma mixing could revise the level structure of these nuclei. One notes that except for ground states and a total of one or two other levels, the bound level structure of the p shell hypernuclei is nonexistent.

### III. Kinematic and Cross Section Constraints

The kinematics of the elementary amplitude in  $(\gamma, K)$  and  $(e; e'K)$  are important not only to define the required experimental apparatus but to determine the relative sticking probability of the recoiling lambda to the nucleus. This probability is, of course, included in the dependence of the hypernuclear cross section as a function of the momentum transfer,  $t$ . In the  $(\gamma, K)$  reaction the minimum momentum transfer is obtained when the angle between the photon and kaon is zero. In a heavy hypernucleus the nuclear recoil energy may be neglected, but the minimum momentum transfer is about 177 MeV/c which is attained at high incident momentum. More typical transfers range from 250 to 450 MeV/c.

In the  $(e; e'K)$  reaction the minimum momentum transfer is attained when the kaon and virtual photon angle is zero. The transition form factor falls off rapidly for  $t > 400$  MeV/c, but may peak at intermediate values of  $t$ . At the peak of the elementary cross section, 1.3 GeV/c, a typical momentum transfer for CEBAF energies is about 300 MeV/c and relatively flat as a function of kaon angle out to about 15°. Kaon distortion effects have been estimated to reduce the theoretical cross sections by 10% in light systems to 60% in heavier systems.<sup>11</sup>

Electromagnetic production of hypernuclear levels will strongly populate unnatural parity states starting from a  $j = 0^+$  nuclear target. This contrasts to hadronic production mechanisms where the spin flip amplitude is small. In addition, since the momentum transfer is large, one would also expect to selectively excite states of high angular momentum transfer.

The above considerations show that for the  $(e;e'K)$  reaction one should use an energy difference between the incoming and outgoing electrons of approximately 1.5 GeV, providing a virtual photon of approximately this energy. In addition, for maximum rate the kaon spectrometer should be placed near the angle of the outgoing virtual photon. If the momentum of the outgoing particles are kept as low as possible then one expects to obtain the best energy resolution for a fixed  $\Delta p/p$  spectrometer system.

If placed at forward angles, the electron spectrometer will limit the luminosity on the target by the singles rate in this detector, which cannot exceed about  $10^8$ /sec. This rate is determined by the necessity to correlate an electron event with a detected kaon. It has been suggested that the electron spectrometer could be placed at zero degrees to take advantage of the enhanced virtual photon flux at these energies.<sup>12</sup> At this angle one would use only  $10^{-3}$  or so of the available beam intensity. If the spectrometer were placed at some finite, but small, angle the decrease in photon flux could in principle be compensated by increased beam intensity. As will be discussed later, and in more detail in Appendix A, one can maximize the rate of hypernuclear formation by placing the electron spectrometer near but excluding a scattering angle of zero degrees, or maximize the signal to noise (accidental) ratio by placing the electron spectrometer at zero degrees.

Because of the high rates envisioned for the electron spectrometer, several methods have been proposed to allow high rates with reduced accidental coincidences. One method is to disperse the beam perpendicular to the bend direction in the spectrometer. This would allow a spatial as well as a time coincidence, and a luminosity increase of a factor of 10 might be possible. This method has the disadvantage of placing more severe constraints on the magnetic spectrometers in order to accept the larger source size. An alternative technique is to use segmented targets

and require the electron and kaon to simultaneously come from the same target. This increases the luminosity by increasing target thickness, but keeps the resolution essentially constant. In this case the spectrometer should have greater longitudinal acceptance.

#### IV. Spectrometer Design

The spectrometer design proposed here (Fig. 2) is based on the premise that resolution in the resulting hypernuclear system is to be optimized. The kaon and electron spectrometers must be moveable to forward angles ( $\geq 5^\circ$ ). This allows thin samples and reduced energy loss which is important to the resolution. At forward angles, the count rate is limited by rates in the electron spectrometer. One expects a low hadronic background in the kaon spectrometer. This facilitates detectors employing particle identification, as well as possible hadronic tagging methods for background and quasi-free suppression of the resulting spectrum.

It is assumed that the beam initially will not be dispersed. This simplifies the spectrometer design, and puts less constraint on the beamline. However, the capability of a dispersed beam is very desirable and this option should be implemented in the future.

Since both the electron and kaon spectrometers are simultaneously required to operate to within  $5^\circ$  of the incident beam, a magnetic dipole is placed at zero degrees to bend the kaons and electrons into their separate spectrometers. The scattered electrons, because of their low momentum, are bent well away from the beam. Unfortunately, the primary beam is also bent by this dipole to an angle of  $4^\circ$ . Thus, the primary beam must be handled properly to ensure it is captured by the beam dump.

We have chosen an incident beam of 1.8 GeV/c, with a virtual photon energy of 1.5 GeV/c. The production cross section tends to peak near this value for reasonable momentum transfers. In addition the energy of all the particles is kept at low values which is important for resolution, and reduces the size of the spectrometers. As shown in Appendix A, if the incident electron beam is kept below 1.8 GeV, the accidental kaon flux in the spectrometer is also kept to a minimum. It is important to keep the length of the kaon spectrometer as short as possible because of kaon decays. Fig. 3 shows the kaon survival ratio per meter as a function of kaon momentum. The central kaon momentum for the design of the kaon

spectrometer was chosen as 1.2 GeV/c with a momentum acceptance of  $\Delta p/p = \pm 60$  MeV/c. Assuming this acceptance then Fig. 4 shows that the electron spectrometer must also have an acceptance of  $\pm 60$  MeV/c which results in a  $\Delta p/p \approx \pm 20\%$  at 300 MeV/c.

#### V. Kaon Spectrometer

The layout of a prototypical kaon spectrometer is shown in Fig. 2. The spectrometer is corrected to 4th order. The spectrometer parameters are given in Table I. Of particular relevance is the acceptance of 14.0 msr and the length of 8 m. A "Raytrace" output for this spectrometer is attached in Appendix D. The beam profile is shown in Fig. 5. The spectrometer bends vertically.

The spectrometer resolution is shown in Fig. 6. The solid curve is the resolution (FWHM) with the  $x-\theta_x$  correlation removed. Other correlations are minor, but can also be applied, further improving the resolution. However, since the actual resolution is then dominated by the spatial resolution of the drift chambers, these corrections will be of little significance. An angular resolution of about 0.5 mr is obtained.

#### VI. Electron Spectrometer

The layout of the electron spectrometer is shown in Fig. 2. The spectrometer is a splitpole magnet designed by H. Enge<sup>13</sup> and presently at the University of Illinois, Fig. 7. In order to achieve the required momentum acceptance ( $\Delta p/p \approx \pm 20\%$ ), Enge has proposed a modification of the magnet poles.<sup>14</sup> A "Raytrace" calculation using the revised magnet parameters is attached in Appendix C. Spectrometer parameters are shown in Table II. This spectrometer must bend horizontally due to the large correlation of  $\theta$  with momentum introduced by the zero degree dipole.

The focal plane for this spectrometer is located near the back face of the magnetic pole piece. Resolution without correction for angle position correlation is about  $3 \times 10^{-4}$  so that only a focal plane detector is needed. Of course, components in the detector package are necessary for timing and particle identification as well as position.

## VII. Particle Tracking and Identification in the Kaon Spectrometer

The particle tracking system in the kaon spectrometer consists of three (x,y) drift chambers of four planes each (to reduce left right ambiguities), placed before the focal plane. These chambers would have a wire spacing of 1cm and should result in a position resolution of about 0.3mm on an (x,y) plane at the position of the focus, as determined by a Monte Carlo calculation. We assume a drift time resolution of about 3ns.

Because it is expected that the ratio of pions and electrons to kaons in the spectrometer will be large, a kaon identification scheme will be required. This system consists of two layers of scintillators (s1,s2), and two layers of Cherenkov detectors ( $c_{\pi}, c_p$ ) and time of flight. The scintillation and Cherenkov detectors are segmented along the focal plane. A coincidence between s1 and s2 indicates a charged particle event and starts the drift time for the chambers as well as opening an ADC gate for the Cherenkov light.

The Cherenkov detectors are designed to separate positive pions,  $c_{\pi}$ , and protons,  $c_p$ . The radiators are selected to detect particles above the velocity thresholds corresponding to the momentum of the particles in question. Of course, all particles with velocities higher than these threshold will also radiate, but for protons, for example, the lucite radiator is designed so that only the light from protons strikes the window surface at an angle less than the critical angle, and thus can escape the radiator. The characteristics of each Cherenkov detector is summarized in Table III.

Essentially, the kaon events are triggered by the signal s1.s2 gated by  $\bar{c}_{\pi} \cdot \bar{c}_p$ . However, under the expected experimental conditions it is quite possible to have more than one track through the electron arm. Therefore, it is necessary to segment the counters and to institute a method to trigger the system on good events. The trigger will be discussed in section XII.

## VIII. Particle Fluxes in the Spectrometers

A knowledge of the background flux of various particles in the spectrometers is necessary to develop the detector system, trigger, and eventual counting rate. We have estimated these rates by the use of relevant experimental data wherever it exists, or, if necessary, by Monte

Carlo calculations from known cross sections. The computer program, "EPC", written by J. O'Connell and J. Lightbody is used to determine the pion and proton flux in the kaon spectrometer.<sup>15</sup> A comparison of the results of this code as modified for multipion production to experimental data is shown in Fig. 8. We are interested in the inelastic electron, and  $\pi^-$  flux in the electron spectrometer; and the  $\pi^+$ ,  $e^+$ , and proton flux in the kaon spectrometer.

We may estimate the lepton flux in both the kaon and electron spectrometers for both bremsstrahlung and pair production. The lepton flux occurs through:

- 1) Bremsstrahlung in which the incident electron scatters into the spectrometer, and;
- 2) Pair production from a virtual photon moving in the direction of the  $e^+e^-$  pair.

The bremsstrahlung flux at forward angles may be determined using the peaking approximation in which a bremsstrahlung photon is emitted along the incident electron direction and the energy degraded electron then Mott scatters from the target. That part of the peaking approximation which corresponds to emission of the photon after scattering is thus ignored. Application of the equations given in Ref. 16 results in a cross section:

$$d\sigma/d\Omega-dp = 4.2\mu\text{b}/\text{Sr-MeV};$$

for a 1.8 GeV incident electron with a 300 MeV scattered electron at  $5^\circ$ . This cross section is consistent with experimental results given in the above publication.

The bremsstrahlung flux at zero degrees may be determined from:

$$dN_e = (X/X_0) \cdot (dE_e/E_\gamma) \cdot N_e;$$

where  $(X/X_0)$  is the target thickness in radiation lengths,  $dE_e$  is the energy acceptance of the spectrometer, and  $E_\gamma$  is the energy of the photon. For a 10mg C target, this results in a rate of  $1.2 \times 10^8/\text{sec}-\mu\text{Amp}$ . Here we have used  $X/X_0 = 2.3 \times 10^{-4}$ ,  $dE_e = 120 \text{ MeV}$ , and  $E_\gamma = 1500 \text{ MeV}$ .

We may also use the virtual photon flux to create an  $e^+e^-$  pair with a flat energy spectrum up to the maximum value of 1.8 GeV. This estimate is given in Appendix B. For the present geometry the cross section to electroproduce a positron into the kaon spectrometer at  $5^\circ$  on a C target is:

$$d\sigma/d\Omega_{\gamma} dp_e = 6\mu\text{b}/\text{Sr-MeV}/c$$

This is comparable to the above approximation for the Bremsstrahlung calculation.

The computer code "EPC" predicts the pion and proton production cross section at 5° on a C target as:

$$d\sigma/d\Omega_{\pi} dp_{\pi}^{+} \approx .03 \mu\text{b}/\text{Sr-MeV}/c$$

$$d\sigma/d\Omega_{p} dE_{p} \approx .0028 \mu\text{b}/\text{Sr-MeV}/c$$

As argued in Appendix A one may maximize the event rate or the signal to noise ratio. We choose to maximize the signal to noise ratio and thus to place the electron spectrometer at zero degrees. For an electron spectrometer acceptance of 120 MeV/c and a bremsstrahlung flux of  $2 \times 10^8$  the incident beam-flux would then be about  $10^{13}$  electron/sec. This produces a kaon rate (see Appendix A), after scaling for the present luminosity, of about 0.4/sec over the entire momentum acceptance of the kaon spectrometer.

The virtual photon flux may be estimated by  $.015 \times N_e \times dE_{\gamma}/E_{\gamma}^{.16}$ . This gives about  $10^{10}$  photons/sec. The positron rate in the kaon spectrometer may be obtained from the cross section estimate obtained previously. Thus,

$$\begin{aligned} N_e &= (6 \times 10^{-30})(10^{13})(6 \times 10^{23}/12)(.01)(.01)(120) \\ &= 3.6 \times 10^4/\text{sec} \end{aligned}$$

The proton and pion flux estimates are similarly:

$$N_{\pi} = 180/\text{sec}$$

$$N_p = 18/\text{sec}$$

## IX. Accidentals

Accidental coincidences will determine the total trigger rate. The singles rate in the electron spectrometer will be about  $2 \times 10^8$ /sec so with a time coincidence of 2ns one expects

$$N_{\text{ACC}} \approx (2 \times 10^8)(2 \times 10^{-9})(0.4) = 0.16/\text{sec}$$

The events will be more or less equally spread over the 120 MeV x 120 MeV energy matrix formed by the electron and kaon spectrometers, so the number of accidentals per 230 keV in binding energy will be:

$$N_{\text{ACC}} \approx / \text{bin} = (0.16)(.23)(7 \times 10^{-5}) = 2.8 \times 10^{-6}/\text{sec}$$

This is probably sufficient for an on-line trigger. Section XII discuss the trigger in more detail.

X. Count Rate for  $^{12}\text{C}(e;e'K)_{\Lambda}^{\text{B}}$

We propose to investigate the spin doublet splittings in p shell hypernuclei in order to further determine the  $\Lambda\text{N}$  interaction. As a representative count rate for such an experiment we present here an estimate of the rate for the production of the ground state of  $^{12}_{\Lambda}\text{B}$ . We assume a beam momentum of 1.8 GeV/c with an inelastic electron at  $0^\circ$  and energy 300 MeV. The kaon spectrometer is placed at its minimum angle of 5 degrees so that the reaction kaon momentum is 1205 MeV/c. The cross section to the ground state of  $^{12}_{\Lambda}\text{B}$  is assumed to be  $50 \times 10^{-33}$  cm<sup>2</sup>/sr. We choose a 10mg/cm<sup>2</sup>  $^{12}\text{C}$  target with a beam intensity of  $10^{13}$  electrons/sec. Using the kaon spectrometer parameters from Table I, and assuming an electron spectrometer of 2 msr acceptance with  $\Delta p/p \approx 20\%$ , the following rate is determined (see section VIII):

$$R = (6 \times 10^{23}/12)(.01)(50 \times 10^{-33})(.014)(1.2 \times 10^{10})(.4)(.8) \\ = 1.3 \times 10^{-3}/\text{sec} \quad (4.8/\text{hr})$$

Here a 40% kaon survival rate and 80% detection efficiency is used. The signal to noise rate is then quite large ( $\sim 400$ ).

XI. Resolution

The kaon spectrometer resolution has been shown to be of the order of 120 keV FWHM. For a 0.01 mg/cm<sup>2</sup> target we expect the following resolution.

primary beam	( $\Delta p/p \approx 10^{-4}$ at 1.8 GeV/c)	180 keV
inelastic electron	( $\Delta p/p \approx 3 \times 10^{-4}$ at 0.3 GeV/c)	90 keV
kaon spectrometer	( $\Delta p/p \approx 10^{-4}$ at 1.2 GeV/c)	120 keV
kaon energy loss	(1.7 MeV/gm/cm <sup>2</sup> ) 30mg/cm <sup>2</sup>	<u>17 keV</u>
	TOTAL	235 keV

However, the dominant resolution contribution comes from the primary beam and only a dispersed beam can reduce this value significantly. The resolution as a function of target mass number is shown in Fig. 9. The sharp rise at small mass is due to angular resolution. It is seen that over most of the mass range the resolution is dominated by the resolution of the primary beam.

## XII. Trigger

Because of the high rates in the electron spectrometer the trigger must be carefully constructed. We propose to segment the electron spectrometer into 60 bins, each covering a momentum bite of 2MeV/c. In addition, the kaon spectrometer would be segmented in 12 bins of 10MeV/c each. Then for a given hypernuclear mass the momentum of the electron and kaon are correlated. For target mass  $\gg$  kaon momentum, a 2MeV/c electron momentum and a 20MeV hypernuclear mass bite require an approximate 18MeV/c kaon momentum bite. Therefore requiring the electron segment to be in coincidence with three kaon segments centered about the kaon segment corresponding to the central value of the hypernuclear mass and electron momentum, all coincident events are captured. This would reduce the accidental trigger rate to:

$$N_{\text{ACC}} = (0.16) \left( \frac{3}{60 \times 12} \right) \times 60 = 0.04/\text{sec}$$

The rate in each electron segment would be  $3 \times 10^6$ . The probability of two events in 4 nanosec, which is twice the resolving time of the electronics, would then be  $\sim .01$ , and the probability of 2 hits or more for any trigger about 0.6. In the off line analysis this multiplicity can be reduced since this rate would be spread over a number of mass bins.

The coincidence trigger may be formed by programmed logic array IC's which would accept, as inputs, the 60 channels of electron segments and the 12 channels of kaon segments. These devices are capable of handling singles rates up to 25MHz and would be preprogrammed for a specific momentum tune of the spectrometers. The coincidence output will form the trigger.

## XIII. Electron Focal Plane Detector

The focal plane detector for the electron spectrometer covers 120 MeV/c in a spatial distance of 80cm giving a dispersion of 150 keV/mm. With a position resolution of 0.6mm this would give an energy resolution of 90keV for the electron arm. If the focal plane drift chambers have a wire spacing of 2.5mm then each wire would have a rate of  $8 \times 10^5$ . Wire

length would be about 10cm. We have previously operated drift chambers with a 2.5mm drift distance at rates of  $10^6$ /wire over a 2cm wire length at Brookhaven National Laboratory. These chambers have an RMS spatial resolution of 0.15mm and a total drift time of about 40nsec. Their time resolution between planes is about 20nsec. Behind the drift chamber would be a set of 60 scintillator segments each covering 2Mev/c. These segments are used for timing information, and consist of two scintillators in coincidence. The rate in each scintillator and the coincidence rate per scintillator segment is  $3 \times 10^6$ . The trigger rate is then equal to the accident rate between the kaon and electron arms or about 0.04/sec.

#### XIV. Timing

It has been proposed that time of flight can be used for particle discrimination between kaons and pions. Over the 8m or so length of the kaon spectrometer the pions and kaons will be separated by about 2nsec. Off line, this information can be used to further exclude pion accidentals, but it would be difficult to implement time of flight in the trigger without imposing additional time structure on the beam. We presently exclude this possibility because the instantaneous rate is already high and the event rate low. Thus, there is little, if any, flexibility left to manipulate the time structure in the beam. Particle identification at the needed level can be accomplished by Cherenkov detectors. The  $\pi/k$  ratio is about 450 (180/0.4).

#### XV. Proposed Measurement And Time Request

We propose to initiate a series of high resolution measurements of electroproduced hypernuclear structure. As previously emphasized, electroproduction will excite both natural and unnatural parity states. Thus, with sufficient resolution, a direct measurement of the spin dependent level structure of p shell hypernuclei can be obtained.

We propose to undertake this program in a series of steps, leading to a high resolution instrument capable of resolving level splittings of the order of a 100kev or so. We believe from the spectrometer studies described above, that such an instrument coupled with a dispersed beam is technically possible, and we are committed its development.

As the first phase of this work we propose to investigate the

characteristics of the electron tagging spectrometer. This would encompass the modification of the Enge splitpole magnet now at the University of Illinois to improve its momentum acceptance. In addition, we propose to secure a dipole for placement at zero degrees in order to separate kaons and electrons, and to build a detector package for the electron spectrometer. We would then investigate the response of this device in an electron beam in Hall C. Rates, backgrounds, resolutions, and target cooling will be investigated. We anticipate beams of no more than  $10^{13}$  electron/sec on target.

The second phase will consist of coupling the electron spectrometer with an existing instrument (probably the SOS) to investigate kaon production and electron-kaon coincidence rates. It is anticipated that the resolution of the hadron arm would be about  $10^{-3}$  which would result in missing mass resolutions of 1 to 2 Mev. These resolutions would be sufficient to measure rates, and test instrumentation, but not sufficient to measure level splittings.

The third phase would be the implementation of a high resolution hadron spectrometer coupled with the electron spectrometer in a way to obtain resolutions on the order of 100kev. This would require a dispersed electron beam on target and perhaps a dispersion matched system. Work on such an instrument is in progress and would continue during the first two phases.

The beam time request is then:

Phase I

Installation of electron spectrometer	
detector package (no beam)	2 weeks
Initial measurement of rates	2 weeks
Measurement of resolution, background	2 weeks

Phase II

Installation of SOS detector package(no beam)	2 weeks
Measurement of kaon rates and a hypernuclear spectrum	3 weeks

The request asks for a split of at least one week during the two runs in Phase I and 6 to 12 months between Phase I and Phase II. It is not possible to presently project a time request for Phase III. Run times would probably be about one week per target.

## XVI. CEBAF Support

The proposal requests that CEBAF provide support in the acquisition and modification of the Enge splitpole magnet as previously discussed. This magnet will require an appropriate power supply. In addition, we request that CEBAF help in the acquisition of a yet to be defined dipole magnet with power supply to act as the kaon and electron separator. As the geometry of this magnet is coupled to the hadron spectrometer it probably would not be the magnet to be used later in the high resolution spectrometer system.

We ask that Hall C be implemented with the ability to disperse the electron beam vertically on target and to dump the deflected zero degree electron beam. A dispersion of about  $8\text{m}/\%$  is adequate. We request engineering help in the final design of the high resolution kaon spectrometer.

Finally, we request that CEBAF provide lab space for the staging and testing of the detector packages, and a computer based data acquisition system.

## REFERENCES

1. W. Brückner, et al, Phys Lett 79B(1978)157.  
R. E. Chrien, et al, Phys Lett 89B(1979)31.  
B. May, et al, Phys Rev Lett 47(1981)1106.
2. P. H. Pile, Proc 5th Int. Conference on Clustering Aspects in Nuclear and Subnuclear Physics, Kyoto, Japan(1988).
3. D. J. Millener, et al, Phys Rev C38(1988)2700.
4. C. B. Dover, private communication.
5. D. J. Millener, et al, Phys Rev C31(1985)499.
6. R. E. Chrien, et al, submitted Phys Rev C.
7. E. H. Auerbach, et al, Ann Phys(N.Y.)148(1983)381.  
A. Gal, et al, Ann Phys (N.Y.)63(1971)63; 72(1972)445; 113(1978)79.  
R. H. Dalitz and A. Gal, Ann Phys (N.Y.) 116(1978)167.
8. M. May, et al, Phys Rev Lett 51(1983)2085.
9. M. Bedjidian, et al, Phys Lett 94B(1980)480.
10. A. R. Bodmer, Phys Rev 141(1966)1386.  
B. F. Gibson and D. R. Lehman, Phys Rev C23(1981)404.
11. T. W. Donnelly and S. R. Cotanch, Proceedings of the 1985 CEBAF Summer Study, Jan 1986.
12. C. Hyde-Wright, et al, Proc of the 1985 CEBAF Workshop.
13. H. Enge, Nucl Inst and Meth 49(1967)181.
14. H. Enge, Private Communication.
15. J. O'Connell and J. Lightbody, Comp in Phys May/June(1988)57.
16. L. W. Mo and Y. S. Tsai, Rev Mod Phys 41(1969)205.

Table I. Kaon Spectrometer Parameters

---



---

Quad length	80 cm
Quad diameter	40.64 cm
Quad field	6 kG (plus higher-order)
Dipole radius	226 cm
Dipole angle	80 degrees
Dipole field	18.06 kG
Dipole airgap	16 cm
Dispersion	8.3 cm/percent
D/M	8.6 cm/percent
Range	$\pm 5$ percent
Solid angle	14 msr
Peak width at waist	0.76 - 2.1 cm
Transverse images	about 2.5 cm
Focal surface	curved, 48 degrees

---



---

Table II. Electron Spectrometer Parameters

---

Momentum	240 - 360 MeV/c
Design central momentum	276 MeV/c
Total length	~ 5 mm
Solid angle acceptance	1.6 msr
Horizontal	25 mr
Vertical	20 mr
Momentum bite	± 2%
Focal plane dimension	
Length	104 cm
Tilt	50°
Horizontal	80 cm
Momentum resolution	$3.8 \times 10^{-3}$

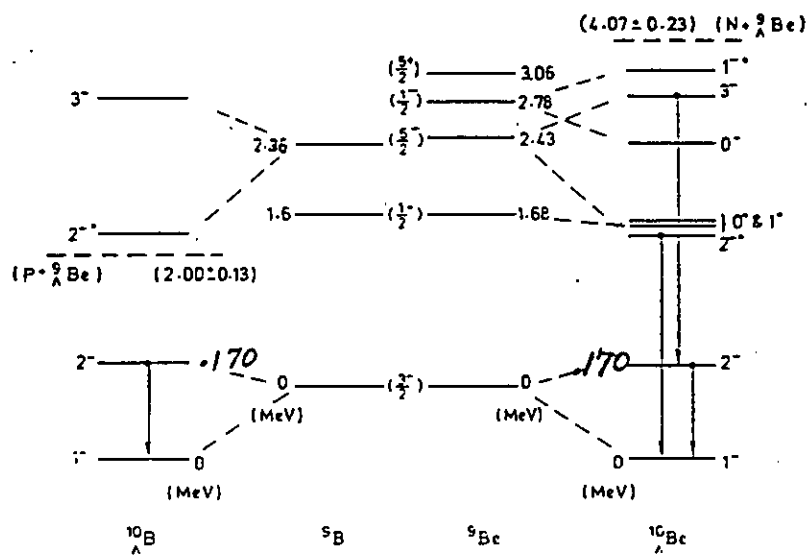
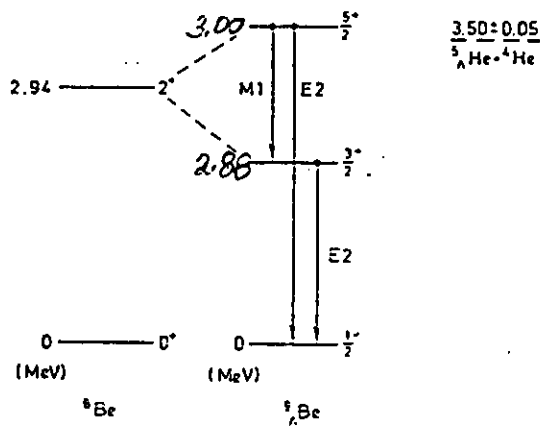
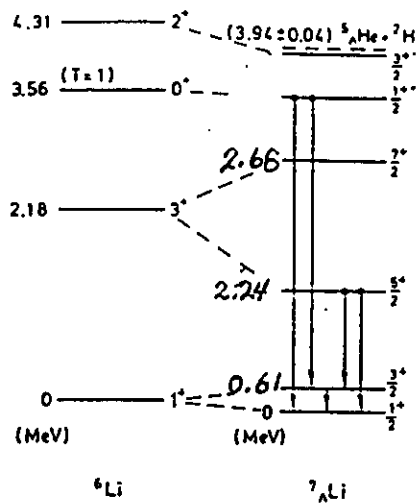
---

Table III. Characteristics of Cherenkov Detectors

Detector	Particle	Radiator	Index	Rejection Rate	k Efficiency Loss
$c_{\pi}$	$\pi, e$	Aerogel	1.07	$10^{-3}$	0.02
$c_p$	p	Lucite	1.54	$2 \times 10^{-4}$	0.02

## FIGURE CAPTIONS

- Fig. 1 - Representative predicted level splittings for p shell hypernuclei
- Fig. 2 - The spectrometer layout for  $(e,e'k)$ . The kaon spectrometer levels vertically.
- Fig. 3 - Kaon survival per meter as a function of kaon momentum.
- Fig. 4 - Kinematics for  $(e,e'k)$  on a C target.
- Fig. 5 - Beam profile for the kaon spectrometer.
- Fig. 6 - Resolution of the kaon spectrometer across the focal plane.
- Fig. 7 - A layout of the Enge splitpole spectrometer.
- Fig. 8 - Comparison of the EPC code to representative data.
- Fig. 9 - System resolution as a function of target mass.





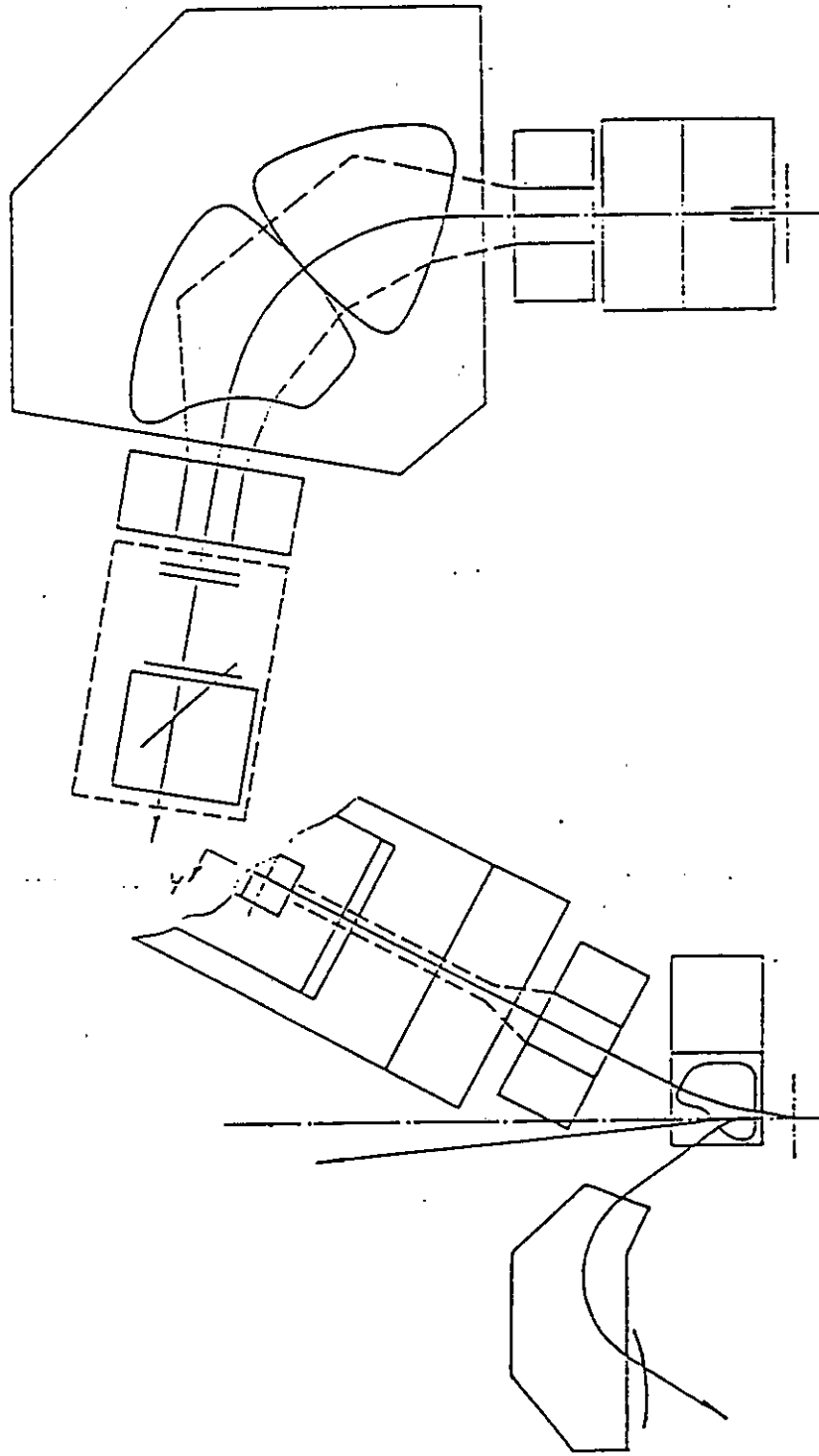
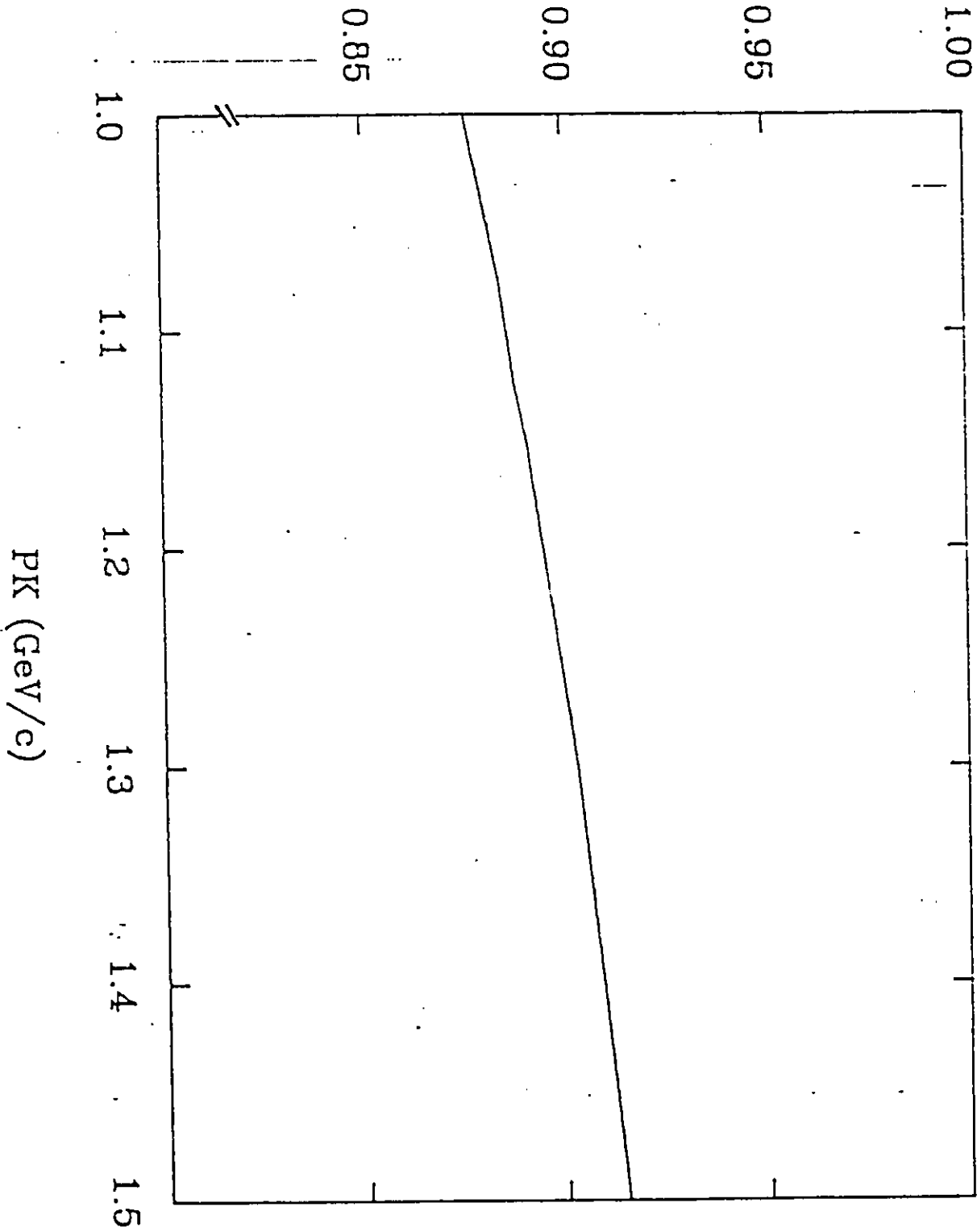
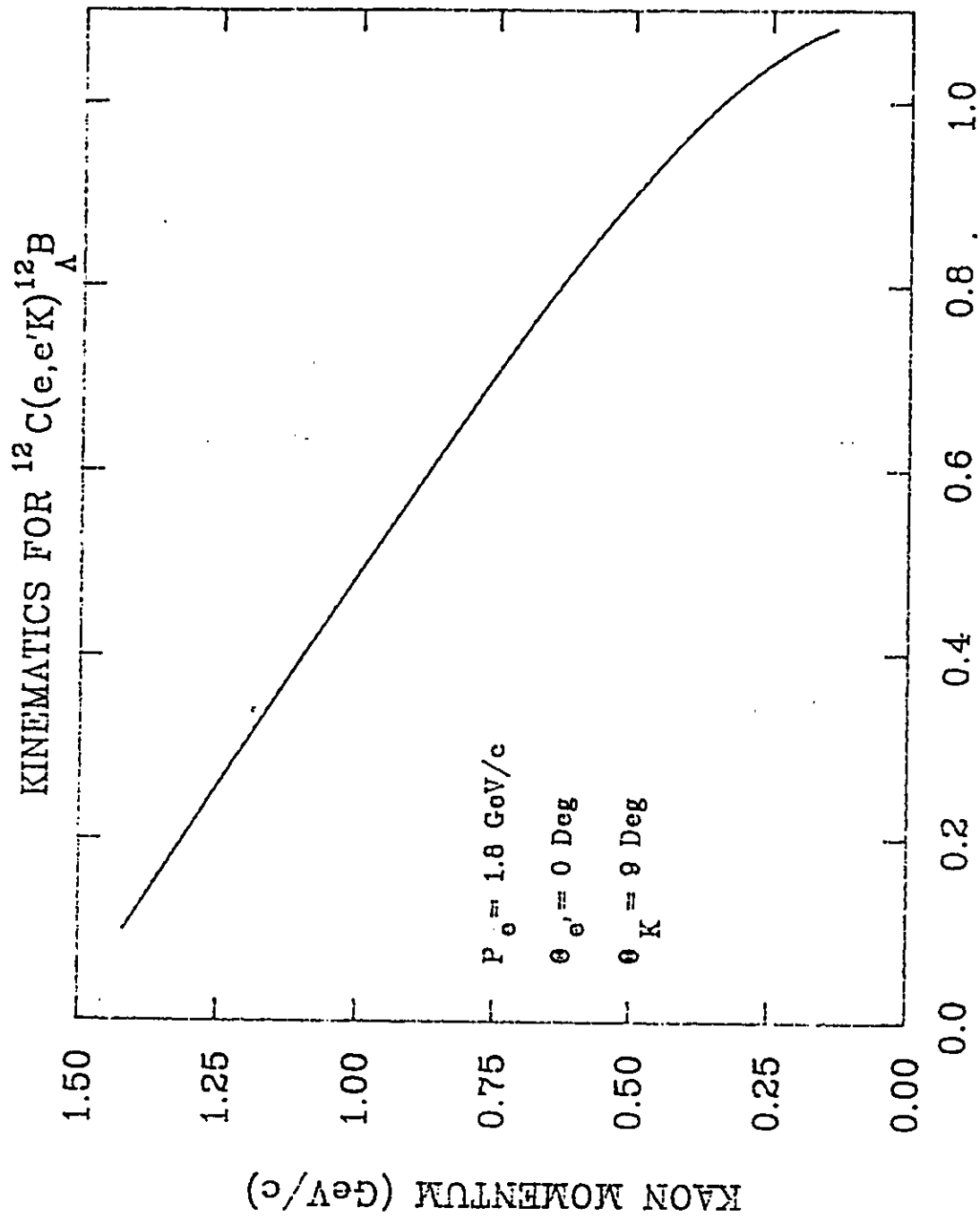


Fig. 2

PROBABILITY PER METER

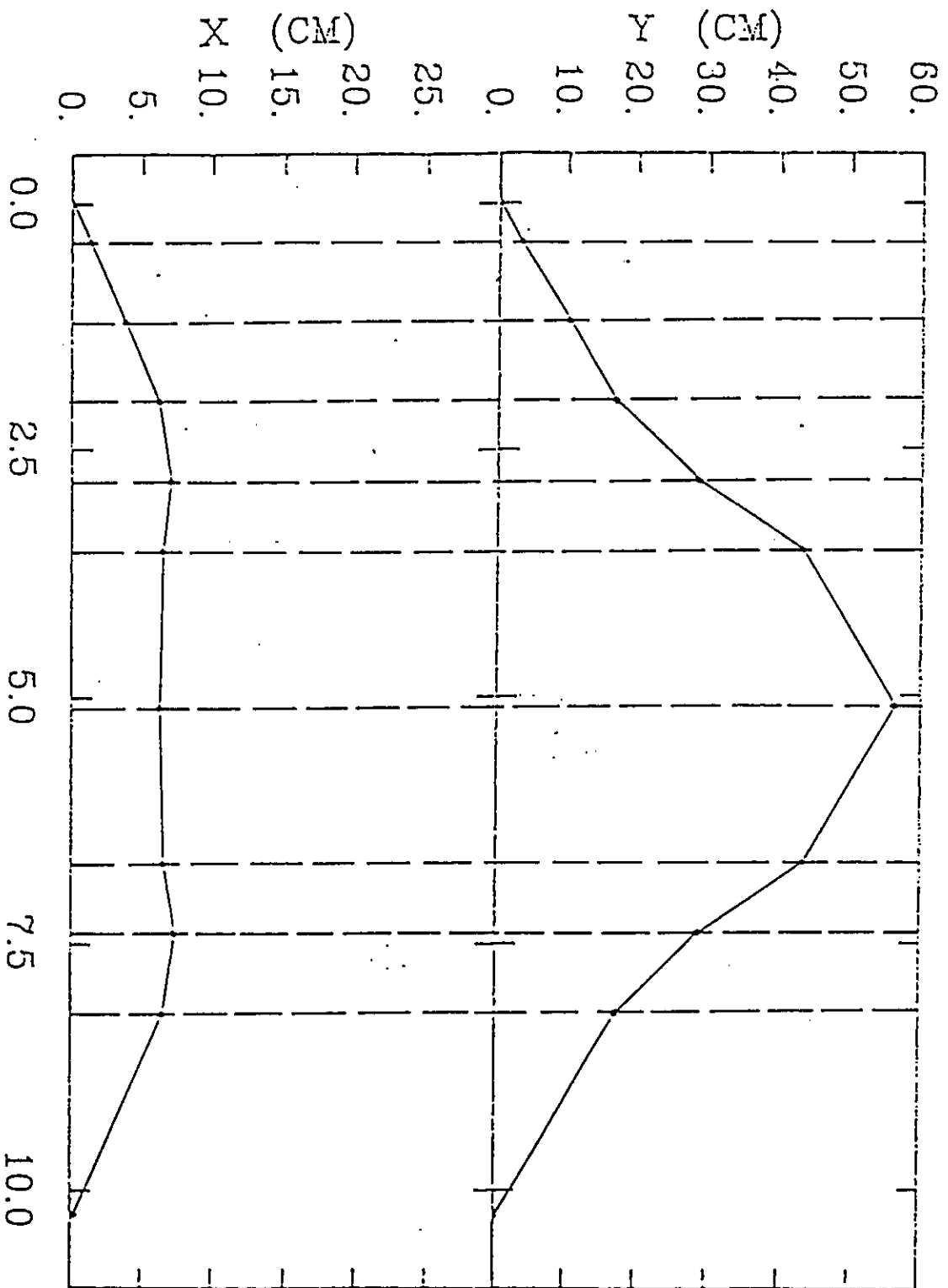
KAON SURVIVAL PROBABILITY





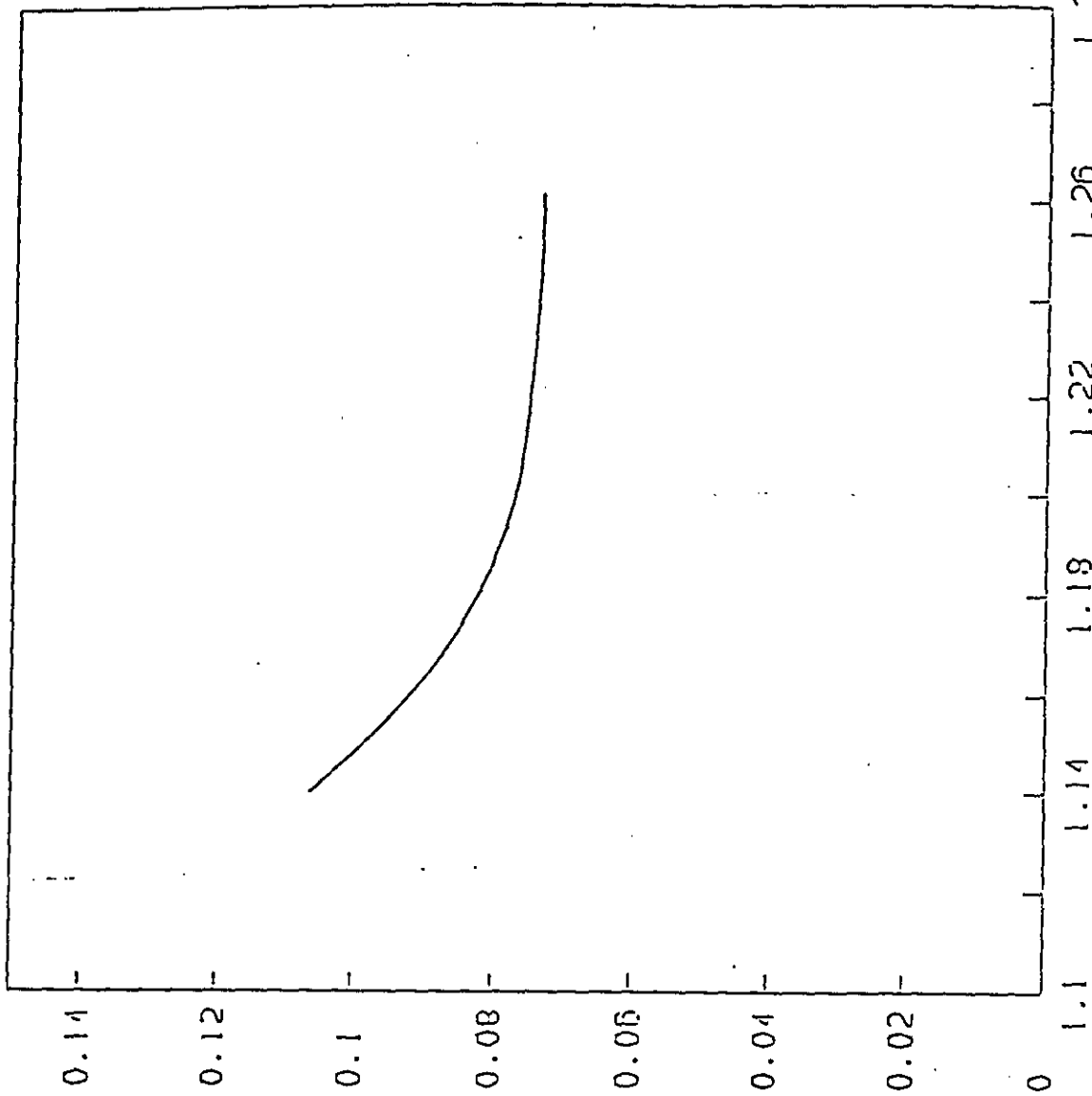
ELECTRON MOMENTUM (GeV/c)

Fig. 4



Z. (METER)

CORRECTED



N = 13 / 27, 11 = 100

RESOLUTION (MeV/c) VS BEAM P (GeV/c)  
STANDARD DEVIATION

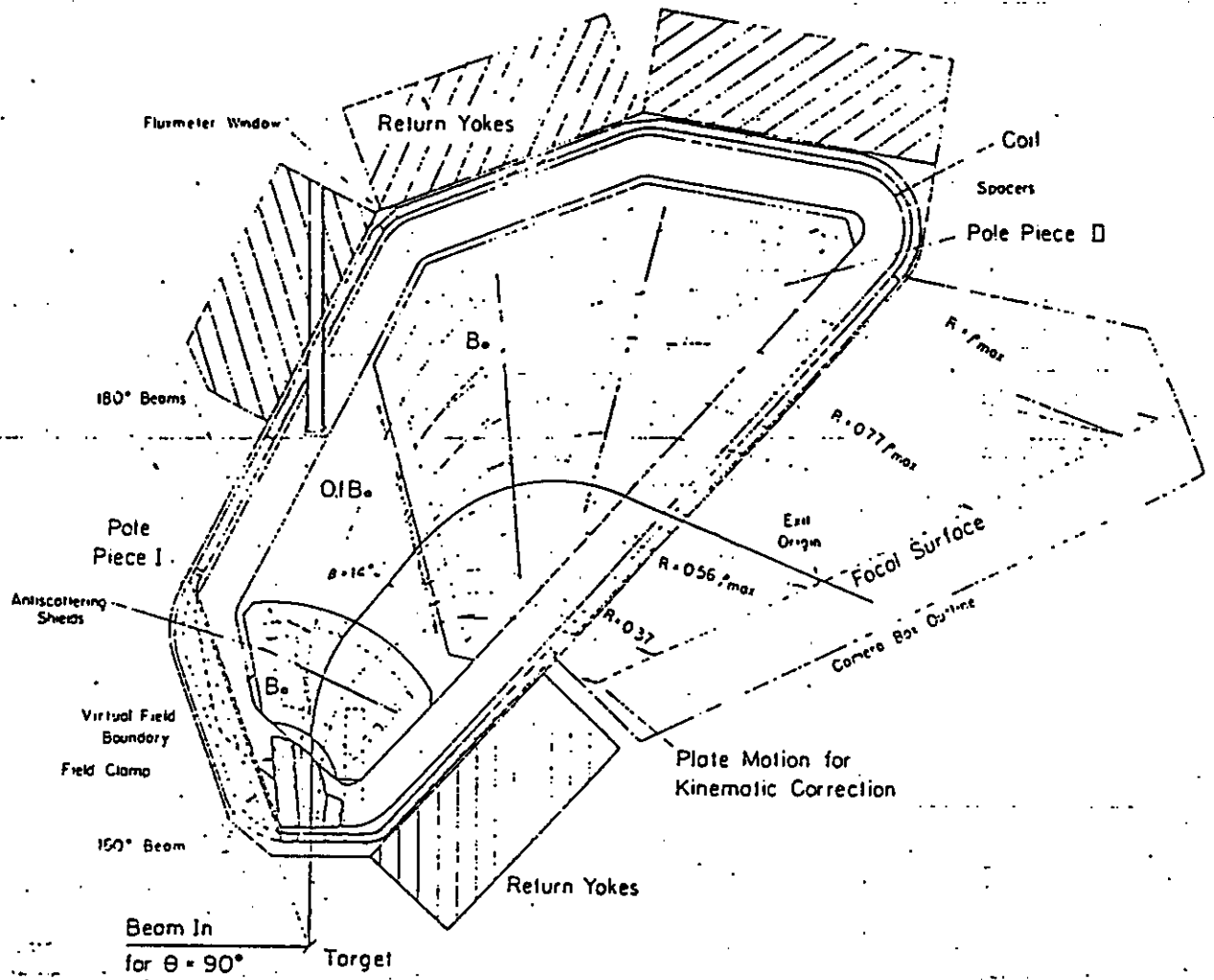


Fig. 7

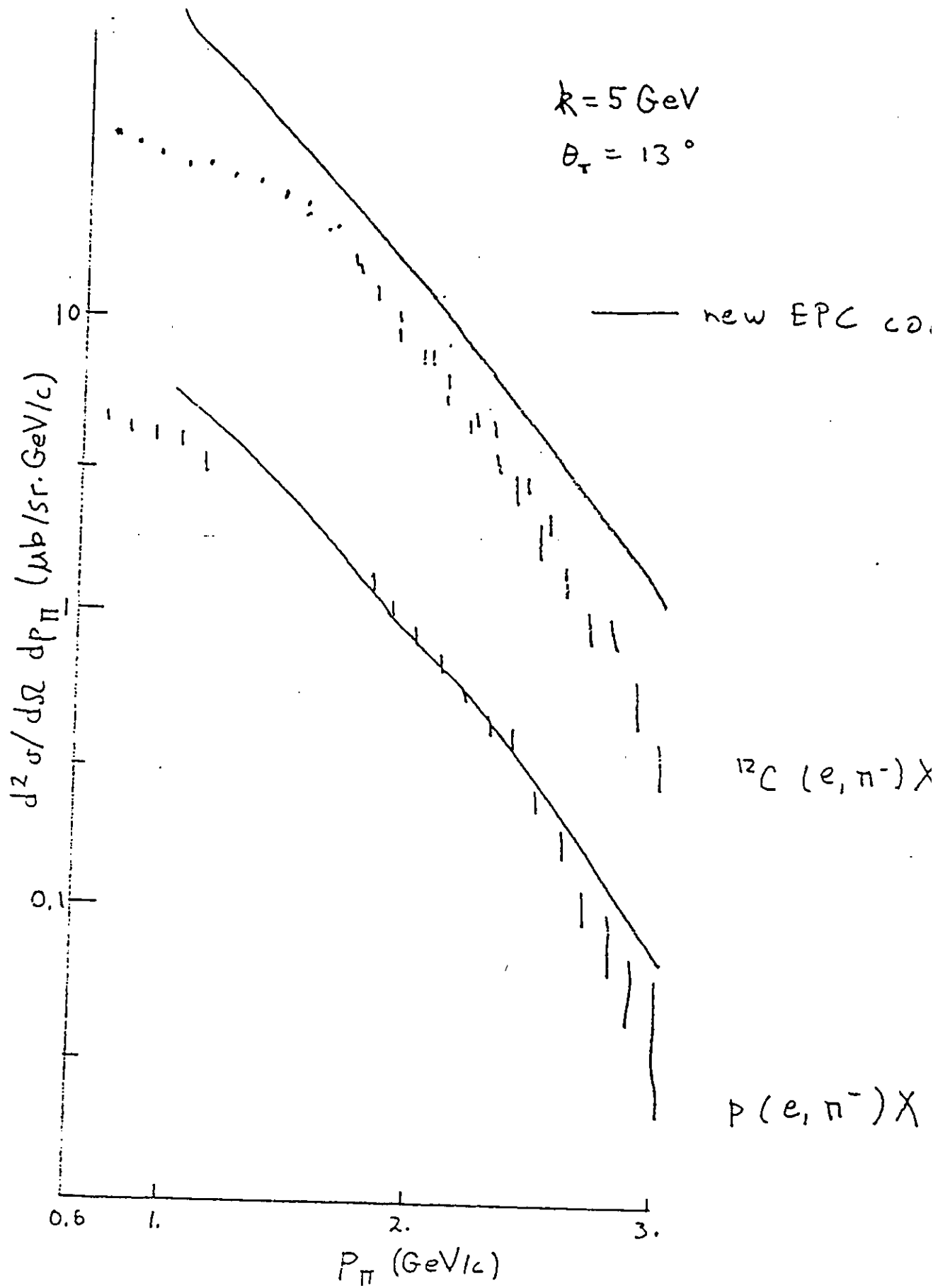


Fig. 8

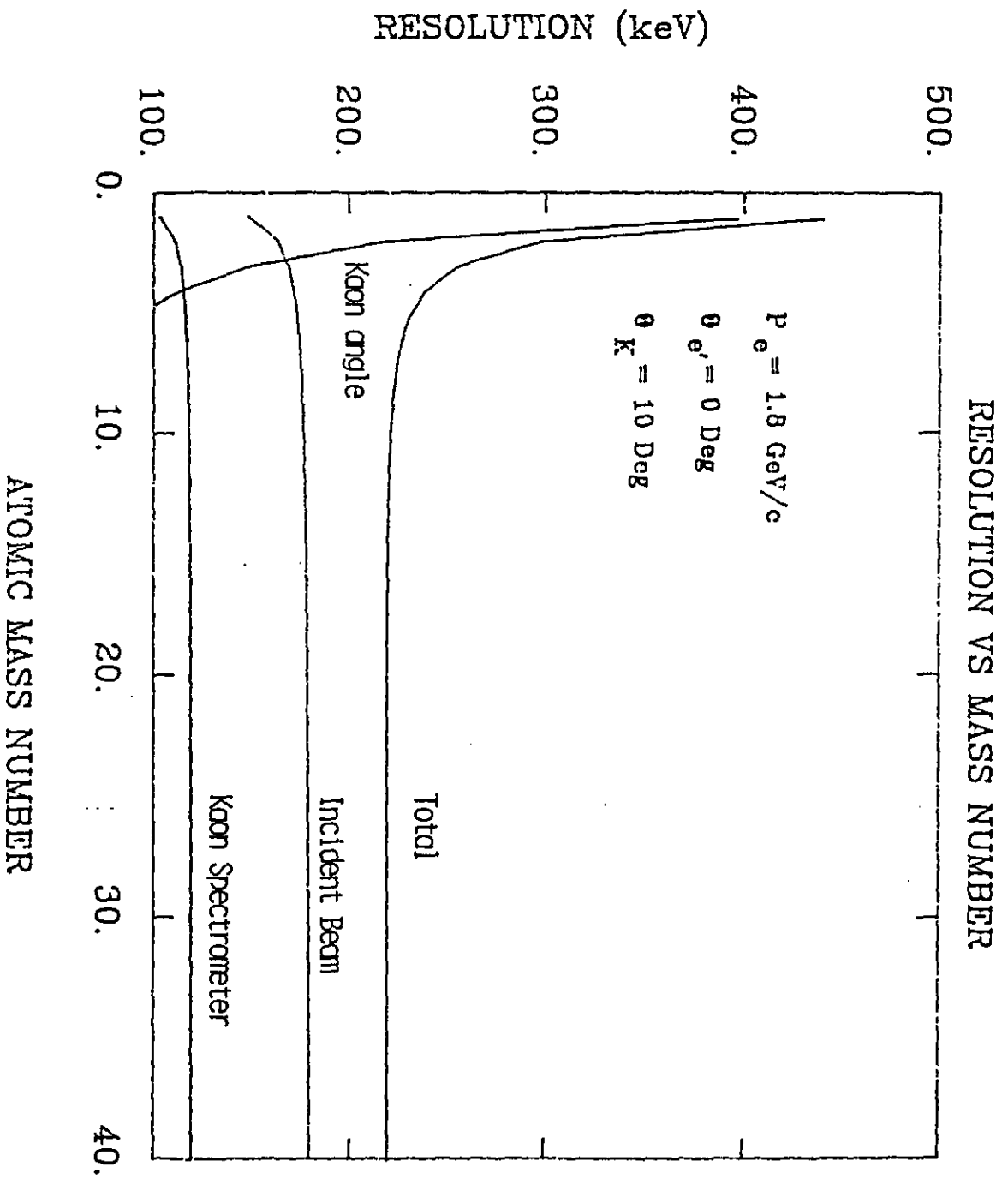


Fig. 9

APPENDIX A

## APPENDIX A

### Kaon Singles Rates in $(e,e'k)$

Ed Hungerford  
University of Houston

#### I. Introduction

Because the  $(e,e'k)$  cross section to specific nuclear states is small, the number of accidental electron-hadron coincidences is important in the design of any experiment. For example, in a configuration optimizing experimental resolution, one must accept high scattered electron rates, while pions, and to a lesser extent protons, will dominate the hadron flux in the kaon spectrometer. Thus, an accurate estimate of the background singles rates in each of the particle spectrometers is crucial to determine the signal to noise event rate. This report describes an estimate of the expected hadron rates in a kaon spectrometer with spectrometer parameters given in Table IA.

#### II. Kinematics

It is assumed that the experiment would be undertaken with an incident electron beam momentum of 1.8 Gev/c with a scattered electron momentum of 300 mev/c. This would produce a virtual photon flux mainly at 0 degrees with an energy of 1.5 Gev. At this energy the  $(\gamma,k)$  elementary cross section is at a maximum; Fig. 1A. However, in order to maximize the hypernuclear event rate, both the electron and kaon spectrometers must be placed at forward angles near zero degrees. As shown in Fig. 2A, the virtual photon angle is confined to forward angles for all electron angles. The selection of the exact forward angle for the electron spectrometer can be considered a separate issue to the background kaon

flux, and may be determined by maximizing the hypernuclear signal, or the signal to noise ratio. However, it is important to realize that selection of the incident and scattered electron energies (the photon energy should be kept near the peak in the elementary cross section) does influence the kaon background rate. If a higher incident and thus scattered electron energy are chosen, both electron and hadron scattering angles may be increased without severe penalty in rate; however, this does open kaon channels other than those producing hypernuclei. In addition, higher energy also adversely effects the resolution for a given spectrometer  $dp/p$ . However, of more concern to this report is the fact that an increase in the kaon singles rate increases the accidental kaon coincidences and event triggers. The required gamma energies to photo-produce kaons in the momentum range of the kaon spectrometer for representative reactions are given in Table IIA. It is clearly important to keep the incident photon energy as low as possible to avoid background production of kaons. This means that the incident electron beam should be low, and a very large energy loss used for the scattered electron.

### III. Cross Sections

The  $(\gamma, k)$  total and differential cross sections are shown in Fig. 3A. These cross sections were fit with Legendre polynomials resulting in the solid curve in the figures. A threshold point of zero cross section was added to the total cross section data. Table IIIA gives the coefficients and  $\chi^2$  per degree of freedom of the fits. The quality of the data is poor, but the fits are reasonable within the statistical error.

#### IV. Quasifree Scattering

The kaon background at low incident electron energies (see Table IIA) from nuclear targets will be dominated by a process in which the kaons are produced by the  $(\gamma, k)$  reaction on quasifree nucleons. In other words, the background is due to a  $N(\gamma, k)Y$  reaction on a bound nucleon,  $N$ , leading to a hyperon,  $Y$ , in the continuum. The rest of the nucleus is then considered a spectator to this reaction. The cross section for the quasifree process may be obtained by modification of the equation derived by de Forest and Walecka<sup>1</sup> for pion electroproduction from a quasifree nucleon. This equation has the form:

$$\frac{d^4\sigma}{d\varepsilon d\Omega_e d\Omega_k dk} = \left( \frac{d^3\sigma}{d\varepsilon d\Omega_e d\Omega_k} \right)_{\text{nucleon}} \frac{p_k}{w_k} R$$

Here  $R$  is the response function of the nuclear medium,  $(\varepsilon, d\Omega_e)$  are the scattered electron energy, and  $(w_k, \vec{k})$  are the kaon (energy, momentum). This approximation uses the lab cross section  $\left( \frac{d^3\sigma}{d\varepsilon d\Omega_e d\Omega_k} \right)_{\text{nucleon}}$ .

The cross section for nuclear electro-production of kaons,  $p(e, e'k)\Lambda$  is then approximated by;

$$\left[ \frac{d^3\sigma}{d\varepsilon d\Omega_e d\Omega_k} \right]_{\text{nucleon}} = \Gamma \left[ \frac{d\sigma}{d\Omega_k} \frac{\sigma_T(p_Y)}{\sigma_T(p_O)} \right]$$

Where  $\Gamma$  is the flux of virtual photons evaluated at zero degrees,  $d\sigma/d\Omega_k$  the photo-production cross section,  $\gamma p \rightarrow k\Lambda$  at  $p_O$ , and  $\sigma_T$  the total cross section for kaon photo-production. The above expression reasonably approximates the angular and momentum dependence of kaon electroproduction from a nucleon.

The virtual flux factor may be obtained from the paper of Hyde-

Wright, Bertozzi, and Finn.<sup>2</sup> Because the virtual flux is sharply peaked near zero degrees, one may approximate the quasifree calculation by putting these photons on the mass shell and assuming all photons are incident at zero degrees in the lab system. Thus the kaon and photon angles decouple, i.e., the kaon angles in the above equation are the laboratory angles. The kaon singles rate may then be obtained by integration of the above equation over the unobserved quantities.

An estimate of the response function may be obtained by use of the Fermi gas model<sup>3</sup> to represent the nucleons in the nucleus. This model states that the number of nucleons with momentum between  $\vec{p}$  and  $\vec{p}+d\vec{p}$  is:

$$N = \rho(p)p^2 dp d\Omega$$

$$\rho(p) = \begin{cases} \frac{3}{4\pi p_F^3} & p \leq p_F \\ 0 & p > p_F \end{cases} ;$$

where  $p_F$  is the Fermi momentum. Using quasifree kinematics and assuming the nuclear recoil is non-relativistic one obtains for R:

$$R = \frac{3Z_e \mu_\Lambda}{4p_F^3 q} p_{\perp F}^2 = \frac{3Z_e \mu_\Lambda}{4p_F q} \left[ 1 - \left( \frac{(w-\epsilon) \mu_\Lambda}{q p_F} - \frac{q}{2p_f} \right)^2 \right] ;$$

where;  $Z_e$  is the nuclear charge,

$p_F$  is the Fermi momentum,

$\mu_\Lambda$  is the effective mass of the  $\Lambda$ ,

$q$  is the momentum transfer,

$p_{\perp F}$  is the Fermi momentum perpendicular to  $\vec{q}$ ,

$w$  is the energy transfer, and

$\epsilon$  is the hyperon-nucleon mass and binding energy difference,

$$\left[ M_H - M_N - (B_H - B_N) \right].$$

The response function has units of inverse energy.

## V. Integration

To determine the number of kaons at a given scattering angle and momentum, the cross section must be integrated over the unobserved scattered electron solid angle. This integration must be carefully handled because of the nearly singular virtual flux factor at zero degrees. The result quoted in Reference 2 is used. As mentioned previously the kaon and electron angles are assumed decoupled so one may proceed directly with this integration.

The fitted differential and total cross sections are inserted and integrated numerically over the unobserved electron energy. Integration limits range from zero to the incident electron energy, but of course there is no contribution to the integral below threshold for kaon production. Again, it is clear that the incident electron energy should be kept as low as possible to reduce the kaon singles event rate in the spectrometer.

Finally, because the rate does not rapidly change as the kaon angle is varied, the total rate may be easily estimated by multiplication of the above integral by the solid angle acceptance.

## VI. Results

The kaon rate in the kaon spectrometer as a function of the kaon momentum is shown in Fig. 4A. This curve is obtained by increasing the  $\Lambda$

quasifree production by a factor of 2 to include production of quasifree  $\Sigma$ 's. Table IA lists the spectrometer specifications used to determine these rates. On average a total kaon flux of 0.4 per second into the 100 MeV/c momentum bite of the kaon spectrometer is obtained. Thus for  $2 \times 10^8$  electrons per second in the electron spectrometer, a 2 nano-second time resolution, and 0.4 kaon per second in the hadron spectrometer; the accidental rate is:

$$N_{\text{Acc}} = (0.4) \times 2 \times 10^8 \times (2 \times 10^{-9}) = 0.16/\text{second}$$

As can be seen from Fig. 4A this is approximately equally distributed over 120 meV of missing mass energy so the number of accidentals per 230 keV mass bin is:

$$N_{\text{Acc}}/\text{bin} \sim (0.16) (0.23) (7 \times 10^{-5}) = 2.4 \times 10^{-6}/\text{sec}$$

These numbers may be compared to those obtained in CEBAF report R-96-013 and the (e,e'k) Letter of Intent. In R-86-013 the calculation used a luminosity which was a factor of 150 less than the luminosity used in the Letter of Intent but the kaon momentum acceptance of the spectrometer was larger. After scaling the rates to the luminosities and spectrometer acceptances assumed here, the comparison in Table IVA is made. Therefore detection of the electrons at zero degrees while resulting in a lower total signal rate, produces a better signal to noise ratio.

Table IA. Requirements for Hypernuclear Spectrometer\*

---

$d\Omega$	10msr
$\Delta p/p$	5%
$dp/p$	$10^{-4}$
$\theta_{\text{scat}}$	$\geq 8^\circ$
$d\theta$	1 mr
$P_{\text{min}}$	1000 MeV/c
$P_{\text{max}}$	1500 MeV/c
length	< 10m
luminosity	$10^{35}$

---

\*Probably needs to be coupled with a  $0^\circ$  horizontal bend to reach the forward angles.

Table IIA. Representative Thresholds for K photo-production from a nucleon with the kaon emitted at 1.2 Gev and 10° scattering angle.

Reaction	Gamma Threshold (Gev/c)
$\gamma_p \rightarrow K\Lambda$	1.55
$\gamma_p \rightarrow K\varepsilon$	1.67
$\gamma_p \rightarrow K^*(892)\Lambda$	1.87
$\gamma_p \rightarrow K\Lambda(1405)$	2.00
$\gamma_p \rightarrow K^*(892)\Sigma$	2.02
$\gamma_p \rightarrow K\Lambda(1520)$	2.20
$\gamma_p \rightarrow \phi(1020)p$	2.30

Table IIIA. Fitted Coefficients for Total and Differential Cross Sections

	l	a <sub>l</sub>
<b>Total Cross Section</b>		
	0	-4.713
	1	2.473
$\sigma_T = \sum a_l p_\gamma^l (\text{GeV}/c)$	2	4.911
	3	-2.2520
	4	-0.410
	5	0.111
	6	-0.009
<b>Differential Cross Section</b>		
$\frac{d\sigma}{d\Omega} = \sum a_l \theta_k^l (\text{degree})$	0	0.28502
	1	0.00389
	2	-0.00005

Table IVA. Comparison of Kaon Single Rates

	CEBAF R-86-013	Scaled Letter of Intent
$N_e$	$2 \times 10^{12}$	$1 \times 10^{14}$
$\rho$	10 mg	30 mg
$d\Omega_k$	35msr	10msr
$(\Delta p/p)_e$	111%	10%
$\epsilon$	.25	.32
# scattered electrons	$10^7$	$10^7$
# kaons/sec-MeV	$7.5 \times 10^{-4}$	$8.0 \times 10^{-2}$ *
scaled # kaons/sec-MeV	$5.9 \times 10^{-4}$	-
scaled # hypernuclear events	$4.4 \times 10^{-4}$	$1.4 \times 10^{-3}$
scaled accidentals/sec-MeV	$1.2 \times 10^{-5}$	$1.6 \times 10^{-3}$
scaled signal/noise(230KeV bins)	160	4

\*9.6  $k^+$ /sec into k spectrometer

## Requirements for Argonne Spectrometer

---

$d\Omega$	10msr
$\Delta p/p$	20%
$dp/p$	$10^{-3}$
$\theta_{\text{scat}}$	$\geq 10^\circ$
$d\theta$	1 mr
$P_{\text{min}}$	100 MeV/c
$P_{\text{max}}$	1500 MeV/c
length	< 10m
luminosity	$10^{38}$

---

#### REFERENCES

1. T. de Forest, Jr. and J. D. Walecka, Adv. in Phys 15 (1966) 1.
2. C. E. Hyde-Wright, W. Bertozzi, and J. M. Finn, Proc of the 1985 CEBAF Workshop.
3. T. W. Donnelly and J. D. Walecka, Ann Rev Nucl Sci 25 (1975) 329.
4. E. J. Moniz Phys Rev 184 (1969) 1154.

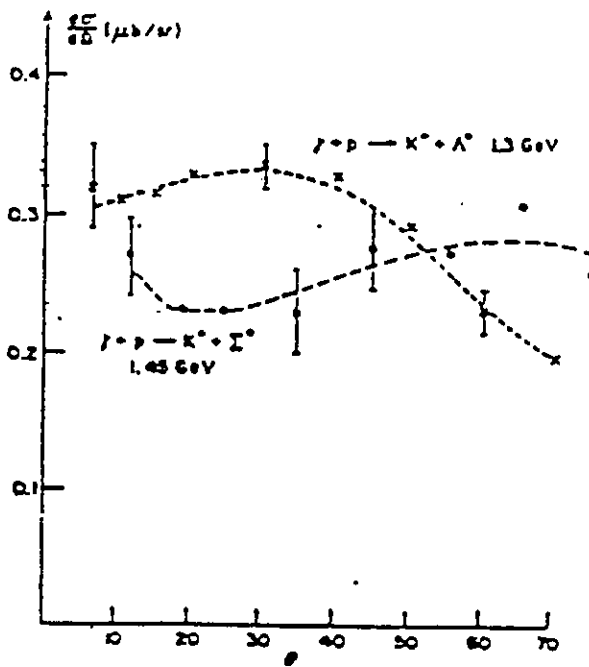
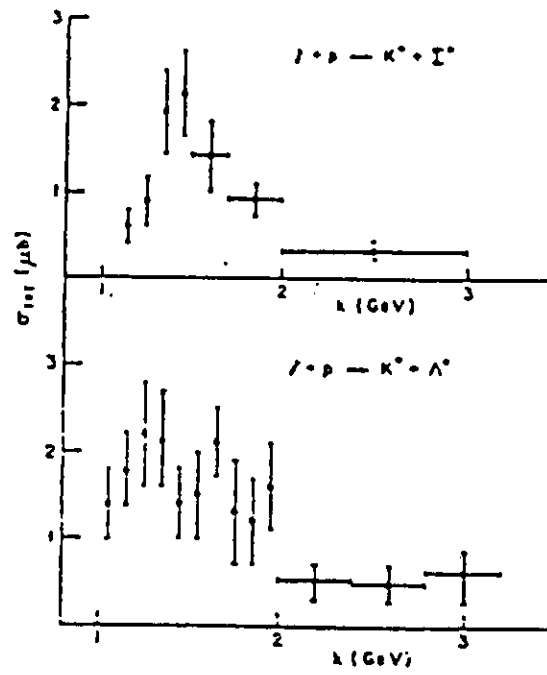
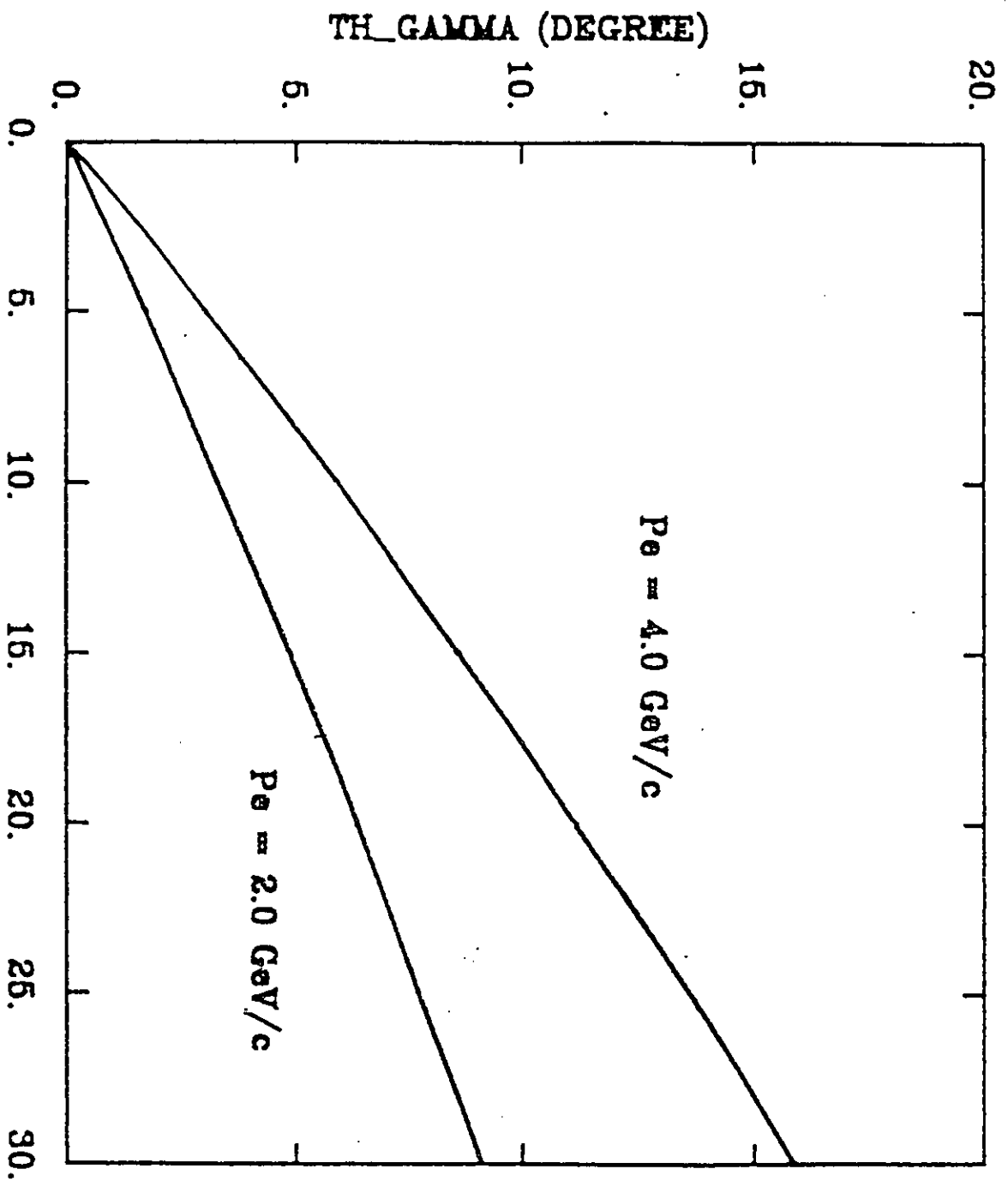


FIGURE 1 A

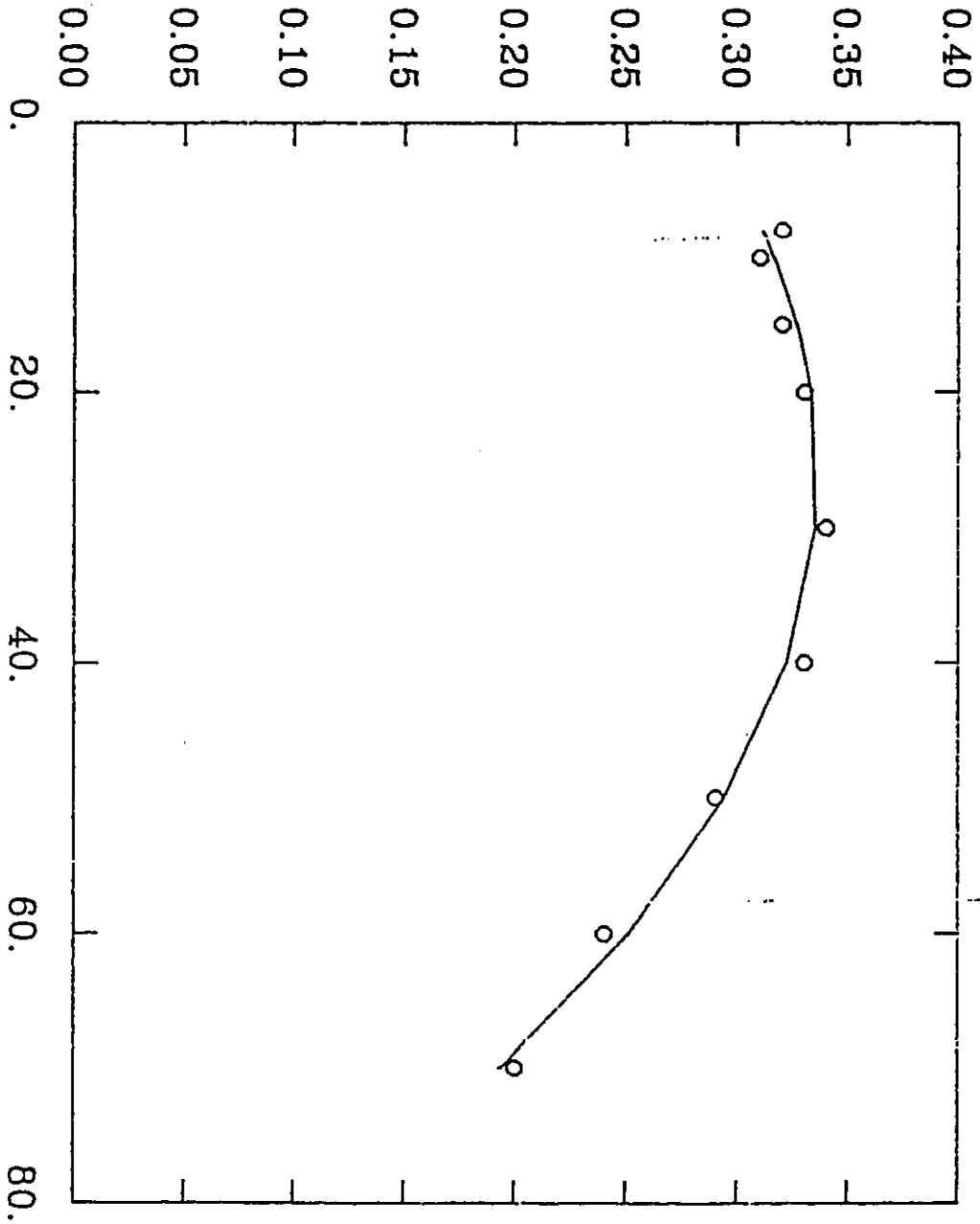
Cross section for  $\Lambda$  and  $\Sigma$  pproduction.



TH\_ELECTRON (DEGREE)

FIGURE 2A

DIFFERENTIAL CROSS SECTION ( $\mu\text{b}/\text{Sr}$ )



KAON ANGLE (DEG)

FIGURE 3A

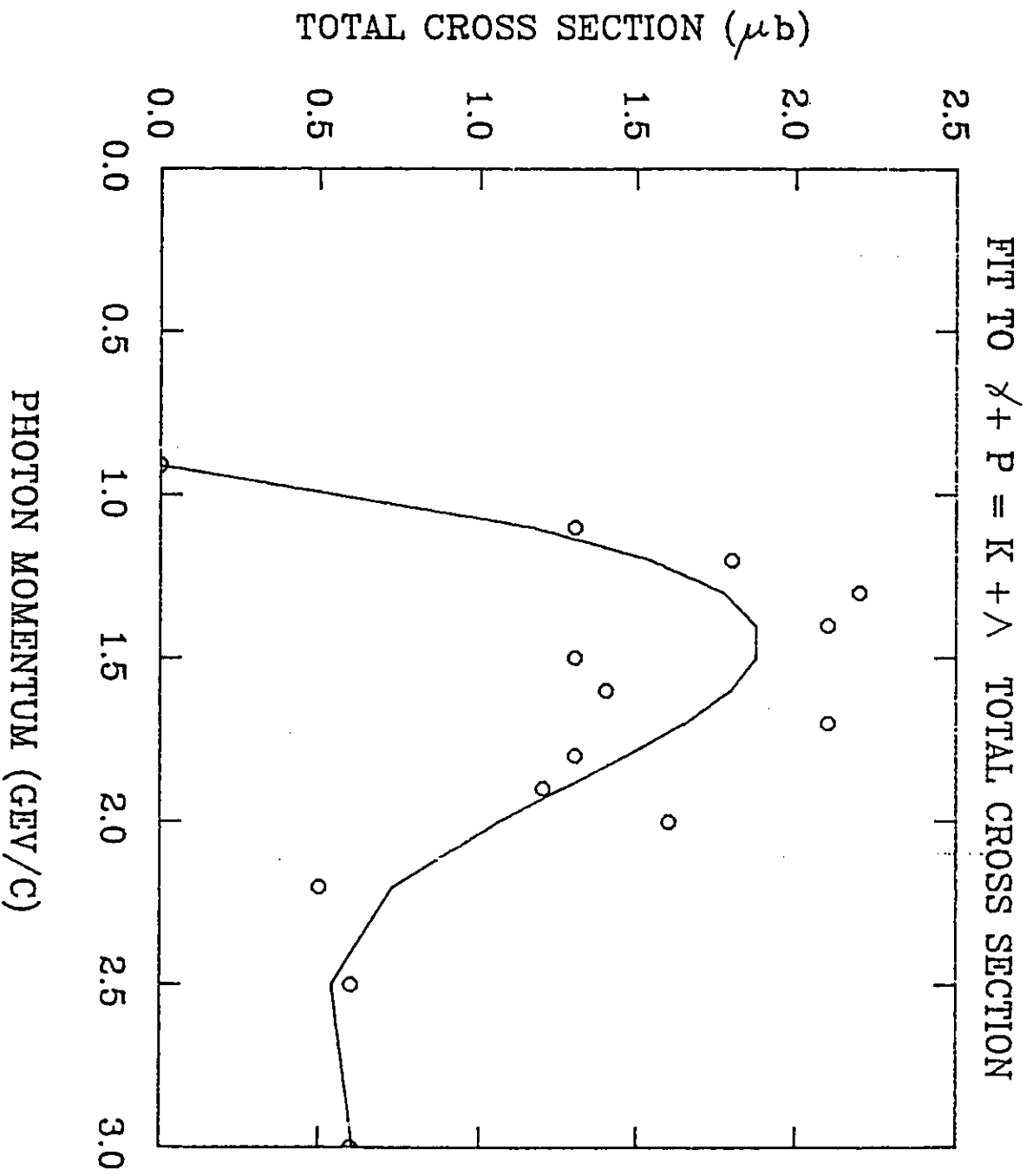


FIGURE 4A

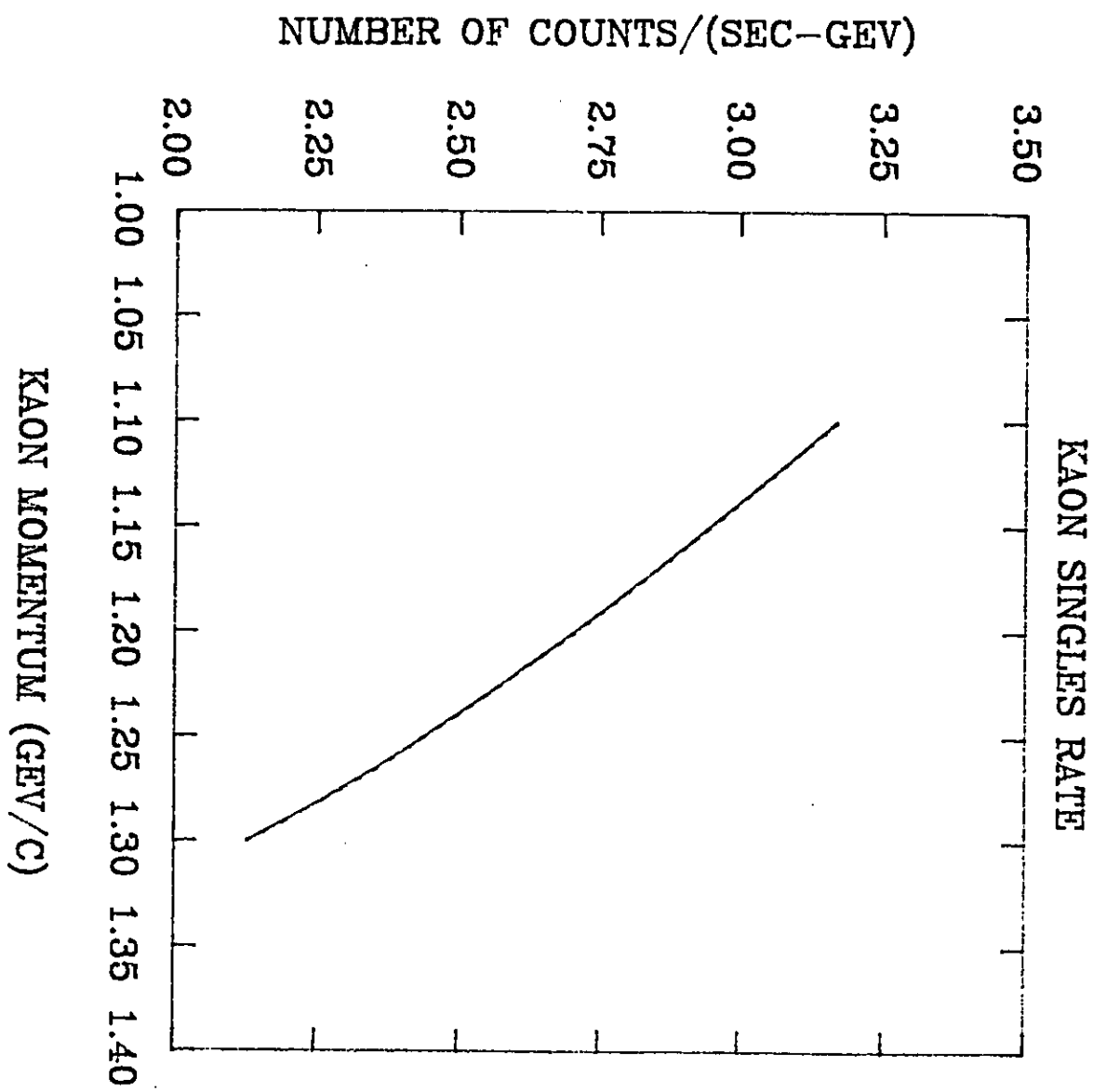


FIGURE 5A

APPENDIX B

## APPENDIX B

### Estimate of the Pair Production Flux

We write the electroproduction cross section in terms of the virtual photon flux and the total cross section for photoproduction of pairs:

$$d\sigma/d\Omega_e dw = \Gamma\sigma_T$$

Here  $d\Omega_e$  is the solid angle for the scattered electron and  $w$  the photon energy,  $(E_0 - E_e)$ , where  $E_0$  is the incident and  $E_e$  the scattered electron energy. The virtual photon flux,  $\Gamma$ , is the number of photons per electron solid angle per photon energy per incident electron and may be obtained from Reference 12. The total cross section for photoproduction is constant for the photon energies considered here, but depends, of course, on the  $Z$  of the target. For  $^{12}\text{C}$  the cross section is about 340 mb/atom.

A photon at energies greater than a few tens of MeV's will produce pairs essentially in the direction of the photon. In addition, a given lepton of the pair has equal probability of production per energy bin. Thus, we will approximate the electroproduction of a lepton by the production of a virtual photon which produce a pair in the same direction as the photon. The production of a positron, for example, at a particular photon angle would be approximated as:

$$\frac{d\sigma}{d\Omega_\gamma dP_{e^+}} = \int_{E_{e^+}}^E dw \frac{\Gamma\sigma_T d\Omega_e}{w \frac{d\Omega_e}{d\Omega_\gamma}}$$

Kinematics give the relation between the electron and photon angles.

$$\sin\theta_e = \frac{P_\gamma}{P_e} \sin\theta_\gamma = \left( \frac{w}{E_0 - w} \right) \sin\theta_\gamma$$

and for  $\theta_e, \theta_\gamma \approx 0$

$$\theta_e = \frac{w\theta_\gamma}{E_0 - w}$$

Therefore, one obtains:

$$\frac{d\Omega_e}{d\Omega_\gamma} = \frac{E_0 - P_e \cos\theta_e}{P_e \cos\theta_e} = \left[ \frac{E_0}{(E_0 - w) \cos\theta_e} - 1 \right],$$

and for  $\theta_e > 0$  but  $\approx 0$

$$\Gamma \approx \frac{\alpha}{4\pi^2\omega} \left[ \frac{E_0^2 + (E_0 - w)^2}{E_0^2 (1 - \cos\theta_e)} \right] \approx \frac{\alpha (E_0 - w)^2}{2\pi^2 w} \left[ \frac{E_0^2 + (E_0 - w)^2}{E_0^2 w^2 \theta_\gamma^2} \right]$$

which results in the cross-section estimate

$$\frac{d\sigma}{d\Omega_\gamma dP_{e+}} = \frac{\alpha\sigma_T}{2\pi^2 E_0^2 \theta_\gamma^2} \int_{P_{e+}}^{E_0} \frac{dw}{w^3} (E_0 - w) [E_0^2 + (E_0 - w)^2]$$

Integration yields

$$\frac{d\sigma}{d\Omega_\gamma dP_{e+}} = \frac{\alpha\sigma_T}{2\pi^2 \theta_\gamma^2} \left\{ \frac{E_0}{P_{e+}^2} - \frac{4}{P_{e+}} + \frac{2}{E_0} \left[ 1 + \frac{3}{2} \ln \left( \frac{E_0}{P_{e+}} \right) \right] + \frac{P_{e+}}{E_0^2} \right\}$$

With the experimental geometry proposed here the final result is:

$$\frac{d\sigma}{d\Omega_\gamma dP_{e+}} = 6.1 \mu\text{b/Sr-MeV/c}$$

APPENDIX C  
Electron Spectrometer

'CEBAF ELEC SPECTROMETER, 300 MEV/C'  
29-SEP-89 11:48:59

RT82.0

PARTICLE ENERGY = 240.0000 MEV  
PARTICLE MOMENTUM = 240.0000 MEV/C  
PARTICLE VELOCITY = 3.00000E+10 CM/SEC  
MASS = 0.0000 AMU